




## Article

# Identification of Co-Deregulated Genes in Urinary Bladder Cancer Using High-Throughput Methodologies

George I. Lambrou <sup>1,2,†</sup> , Kleanthis Vichos <sup>2,3,†</sup>, Dimitrios Koutsouris <sup>2,\*</sup>  and Apostolos Zaravinos <sup>4,\*</sup> 

<sup>1</sup> First Department of Pediatrics, Choremeio Research Laboratory, National and Kapodistrian University of Athens, 15127 Athens, Greece; glamprou@med.uoa.gr

<sup>2</sup> School of Electrical and Computer Engineering, Biomedical Engineering Laboratory, National Technical University of Athens, 15780 Athens, Greece; kle.vichos@gmail.com

<sup>3</sup> School of Electrical and Computer Engineering, University of Patras, 26504 Patras, Greece

<sup>4</sup> Department of Basic Medical Sciences, College of Medicine, Member of QU Health, Qatar University, Doha 2713, Qatar

\* Correspondence: dkoutsou@biomed.ntua.gr (D.K.); azaravinos@qu.edu.qa (A.Z.); Tel.: +30-210-7467427 (D.K.)

† Co-first authorship.

**Featured Application:** Urinary bladder cancer (UBC) is the second most common urogenital solid tumor and the eleventh in the rank among all types of solid tumors. Although several oncogenes and tumor suppressors are known to be implicated in the disease, the list of candidate prognostic markers has recently expanded, as a result of the power of new high-throughput methodologies. The prognosis and therapy of UBC have progressed greatly during the last years. However, a majority of the different tumor subtypes still relapses, manifesting poor prognosis. Here, we identified gene expression patterns being common across different histological phenotypes of UBC. Such an approach could be useful in the discovery of prognostic and therapeutic targets able to be applied in the majority of the tumor's subtypes.



**Citation:** Lambrou, G.I.; Vichos, K.; Koutsouris, D.; Zaravinos, A. Identification of Co-Deregulated Genes in Urinary Bladder Cancer Using High-Throughput Methodologies. *Appl. Sci.* **2021**, *11*, 1785. <https://doi.org/10.3390/app11041785>

Received: 25 September 2020

Accepted: 23 November 2020

Published: 18 February 2021

**Publisher's Note:** MDPI stays neutral with regard to jurisdictional claims in published maps and institutional affiliations.



**Copyright:** © 2021 by the authors. Licensee MDPI, Basel, Switzerland. This article is an open access article distributed under the terms and conditions of the Creative Commons Attribution (CC BY) license (<https://creativecommons.org/licenses/by/4.0/>).

**Abstract:** Although several genes are known to be deregulated in urinary bladder cancer (UBC), the list of candidate prognostic markers has expanded due to the advance of high-throughput methodologies, but they do not always accord from study to study. We aimed to detect global gene co-expressional profiles among a high number of UBC tumors. We mined gene expression data from 5 microarray datasets from GEO, containing 131 UBC and 15 normal samples. Data were analyzed using unsupervised classification algorithms. The application of clustering algorithms resulted in the isolation of 6 down-regulated genes (*TMP2*, *ACTC1*, *TAGLN*, *MFAP4*, *SPARCL1*, and *GLP1R*), which were mainly implicated in the proteasome, base excision repair, and DNA replication functions. We also detected 6 up-regulated genes (*CDC20*, *KRT14*, *APOBEC3B*, *MCM5*, *STMN*, and *YWHAB*) mainly involved in cancer pathways. We identified lists of drugs that could potentially associate with the Differentially Expressed Genes (DEGs), including Vardenafil, Pyridone 6, and Manganese (co-upregulated genes) or 1D-myo-inositol 1,4,5-triphosphate (co-down regulated genes). We propose 12 novel candidate markers for UBC, as well as potential drugs, shedding more light on the underlying cause of the development and progression of the disease.

**Keywords:** urinary bladder cancer; microarray; common gene expression; unsupervised machine learning algorithms

## 1. Introduction

Urinary bladder cancer (UBC) is the second most common cancer of the human urogenital system [1–5]. In the United States alone, it is the sixth most common malignancy representing 4.6% of all cancers, while globally it ranks eleventh in frequency [2–5]. The tumor's diagnosis is not related to age, yet its occurrence is very rare before the age of 40,

with an average diagnosis at 65–70 years [2–5]. The male to female ratio is approximately 4:1. In men, UBC is the seventh most frequent tumor preceded by those of the prostate, lung, and colon. Differences in male to female ratio are probably attributed to the gender-related life-style, to the effect that androgenic hormones have, compared to estrogens, as well as to the process of oncogenesis in the bladder [2–5].

Depending on their histological type, urinary bladder tumors are classified into transitional cell carcinomas (TCC, 95%), squamous cell carcinomas (SqCC, 1–2%), adenocarcinomas (1%), and small cell carcinomas (SmCC, <1%). Finally, there are even rarer forms, of epithelial or non-epithelial origin, such as leiomyosarcoma, lymphoma, carcinosarcoma, and rhabdomyosarcoma [6]. The staging and grading of the tumor are both critical parameters for the likelihood of its recurrence and progression. Although both give an overview of the disease state, they have limited prognostic capacity in terms of the recurrence of the tumor, patient survival, or response to treatment. Therefore, efforts are constantly made to detect new biomarkers (genes), using a sufficient sample of cancer patients of different tumor stage and grade [1,4,5,7].

Several genes are well-known to participate in the malignant transformation of cells in UBC. These include proto-oncogenes, which once aberrantly expressed, interfere with normal growth mechanisms. The best example of this case is the *RAS* family of genes, which encode a group of proteins (P21 or G) that indirectly regulate cell growth, where *RAS* mutations lead to uncontrolled cell growth [8,9]. Other known oncogenes include *MYCC* [10], *HER2* (Cerb-B2) [11], *MDM2* [12], *FGFR3* [13,14] and *ERBB1* [15–17]. Several cycle-regulatory genes are also involved in the onset of the disease.

DNA microarrays constitute a high-throughput technology used for the study of gene expression patterns. Common applications of microarrays include the study of changes in gene expression between different conditions [18]. The present work compares two different classes, healthy tissue used as controls and tumors from all stages and grades of the urinary bladder.

The determination of gene relationships or groups of genes and the identification of biological functions of interest is carried out using machine learning algorithms, such as clustering and classification [18]. A major challenge in the analysis of gene expression is the manipulation of the large number of genes found in the original dataset, which could be up to tens of thousands. Many of these genes are not related to grouping or classification and therefore, the data must be adapted somehow, to enhance the relationship between genes and samples. Data (genes) that do not provide any additional information, will add significant complexity to the study, if not removed [19]. For example, if the expression of a particular gene is the same in all samples, this gene will consequently not be able to distinguish between sub-groups. Conversely, if a gene is expressed differently, e.g., between control-disease groups, then, it is probably useful for the distinction. Therefore, the selection of an optimal gene identification subset from the original dataset is an important step before grouping or classifying, and it is customary to call such a subset of genes, “differentially expressed genes” (DEGs) [19]. In the present work, we utilized computational methods, aiming to detect common gene expression patterns in UBC, among different subtypes of the tumor. We have previously used a similar approach, through which we identified that *CDC20* is a possible gene marker for the disease [20,21]. Here, we expanded our investigation by collecting gene expression data from various UBC subtypes and detected more candidate genes, which were commonly deregulated across them. Importantly, we validated most of these in an independent sample cohort. Our hypothesis is that gene expression should manifest common profiles across urinary bladder cancers, despite their histological differences. Although gene expression profiling has been widely used for tumor sub-classification, our attempt is to use it in order to find common expressional profiles, and therefore, common prognostic and/or therapeutic targets.

## 2. Materials and Methods

### 2.1. Dataset Collection

We mined gene expression data from five distinct datasets all freely available in the Gene Expression Omnibus (GEO) database of the National Center for Biotechnology Information (NCBI, Bethesda, MD, USA). All data derived from gene expression DNA microarray experiments were performed on the tissues of patients with bladder cancer (disease samples), as well as on healthy tissues (control samples) (Supplementary Table S1). In particular, the collected datasets were GSE27448 (consisted of 10 UBC and 5 control samples), GSE89 (consisted of 40 pathological samples), GSE3167 (consisted of 41 pathological samples and 19 controls), GSE7476 (consisted of 9 pathological samples and 3 controls) and GSE12630 (consisted of 19 pathological samples). The aforementioned datasets were selected on the basis of tumor type, i.e., UBC samples representing a complete spectrum of subtypes (e.g., Ta, Tis, T1, muscle-invasive, metastatic, grade 1–4). In total, we collected gene expression data from 131 cancer samples and 15 control samples and analyzed them computationally.

### 2.2. Data Pre-Processing

The aforementioned datasets were produced by different microarray platforms, whereas each platform contained a different number of probes ranging from 7000–50,000. In order to create a common gene dataset, present across all microarray platforms, the “annotation tables” of all platforms were used, in which the detailed information of each probe was available. Gene IDs and the corresponding gene symbols were used as the common identifiers for gene selection, as these are the official identifiers listed on the NCBI website. For example, the gene with the official gene symbol TP53 has a gene ID# 7157. This final selection of genes based on the above criteria resulted in 2266 common genes among all experiments.

### 2.3. Background Correction and Normalization

Background correction was performed as previously described [20,21]. Normalization was implemented using quantile normalization [20–24]. Both were executed in the Matlab<sup>®</sup> computational environment (The Mathworks Inc., Natick, MA, USA).

### 2.4. Differentially Expressed Genes (DEGs)

To evaluate the DEGs between UBC and control samples, a permutation test with 10,000 iterations for each gene was utilized with *t*-statistic with unequal variance. The estimated *p*-values were calculated based on the common distribution of all calculated *t*-scores derived from all permutations for each gene. So, in total we calculated  $10,000 \times 2266$  *t*-scores, thus the minimum *p*-value that could be obtained was  $1/(10,000 \times 2266) = 4.4 \times 10^{-8}$ . Applying previous algorithms [25], based on the distribution of *p*-values, we also estimated the coefficient  $\pi_0 = m_0/m$ . This gives an approximation of how many genes are truly null, i.e., not differentially expressed. Therefore, approximately  $0.4169 \times 2266 = 944.69$  genes were not differentially expressed. Therefore, if all genes were selected this would result in a false discovery rate (FDR) equal to 41.6%. In addition, the above algorithm derives the *q*-value for each gene. Based on these, we obtained the corresponding FDR value for all the genes that were considered to be statistically significant (Supplementary Figure S1). Based on the FDR, one can select the *q*-value (hence the *p*-value cutoff) and at the same time, examine the number of false positives [25].

Consequently, by choosing a cutoff *p*-value = 0.01, we obtained a *q*-value = 0.021; i.e., FDR = 2.2% and thus, 440 genes were selected as differentially expressed, among which, 9.4 false positives are expected (Supplementary Figure S2). The final calculated parameters were  $m = 2266$ ,  $m_0 = 944.7$ ,  $S = 440$  and  $F = 9.4$ , FPR (false positive rate) was equal to  $9.4 / 944.7$  (1%), specificity =  $1 - \text{FPR} = 99\%$ , FNR (false negative rate) =  $67.4\%$  and sensitivity =  $1 - \text{FNR} = 32.6\%$ . The results are summarized in Supplementary Table S2.

### 2.5. Unsupervised Classification Methods

We used unsupervised machine learning classification algorithms, which included hierarchical clustering (HCL) with the unweighted pair group method with arithmetic mean (UPGMA) and k-means clustering. Both methodologies were applied to the set of DEGs, in order to unravel expression patterns, as well as common expressional profiles across all UBC samples. The k-means algorithm was applied with 100 iterations and the optimal cluster number for the k-means algorithm was estimated using the Calinski–Harabasz criterion. We complementarily used the Davies–Bouldin algorithm for detecting the optimal number of clusters [26].

### 2.6. Common Expression Patterns in UBC

The DEGs were examined for taking part in possible common expression patterns, i.e., genes that were either down- or up-regulated across all UBC samples, irrespectively of the tumor diagnosis. The clusters revealed by unsupervised classification were examined separately. Each gene was counted for its occurrences in up- or down-regulation across all samples and the result was divided by the total number of samples, providing the percentage of up- or down-regulated samples for the respective gene. We looked for genes that were co-up or down-regulated, either across all UBC samples (100%), or in 90–99% of them, respectively.

### 2.7. Gene Ontology (GO) Enrichment

GO enrichment was performed using gprofiler [27] and WebGestalt [28–31]. Gene definitions and functions were based on the databases of the National Institute of Health (NIH, Bethesda, MD, USA).

### 2.8. Inter-cohort Validation of the DEGs

We validated the top deregulated genes using expression data from the Cancer Genome Atlas Bladder Cancer (TCGA-BLCA) dataset, composed of 404 urinary bladder cancer samples and 19 normal bladder samples. To increase the number of the normal samples, we also used 9 normal samples from the GTEx project, having a total of 28 normal bladder samples. We used  $\log_2(\text{TPM} + 1)$  to log-scale the expression values and the one-way ANOVA to assess statistical differences between bladder cancer and normal samples from both the TCGA and GTEx projects. A  $\log_2\text{FC} = 1$  and a  $p = 0.01$  were used as cutoff thresholds for statistical significance.

## 3. Results

### 3.1. HCL of DEGs

The DEGs were initially clustered using HCL, to detect patterns of expression. Interestingly, we found a cluster of genes exhibiting global down-regulation across all cancer samples. In addition, high grade and metastatic tumors were clustered together, as well as grade 4 tumors clustered with Ta/T1 grade 3 ones. T1/T2 grade 2 and grade 3 cancers, also appeared to manifest common patterns of gene expression (Figure 1).

### 3.2. K-Means of DEGs

To investigate further the profile of the DEGs, we clustered them using k-means (Figure 2). We broke-down the globally DEGs and separated them. In particular, the Davies–Bouldin criterion manifested that the optimal numbers of clusters were 2, 3 and 4 (Figure 2A). Clustering for  $k = 2$  (Figure 2B) manifested two clusters, where the first included 49 genes and the second 391 genes. The first cluster showed probable candidate genes for global down-regulation, while the second manifested a variety of gene expressional profiles. Therefore, we clustered genes for  $k = 3$  (Figure 2C) and  $k = 4$  (Figure 2D). For  $k = 3$ , the first cluster remained the same and the next two clusters manifested up-mid, up- and down-regulated genes (Figure 2C). A further separation with  $k = 4$ , still manifested the cluster



with the possible 49 down-regulated genes, while it revealed a cluster of 278 genes with possible up-regulated genes (Figure 2D).

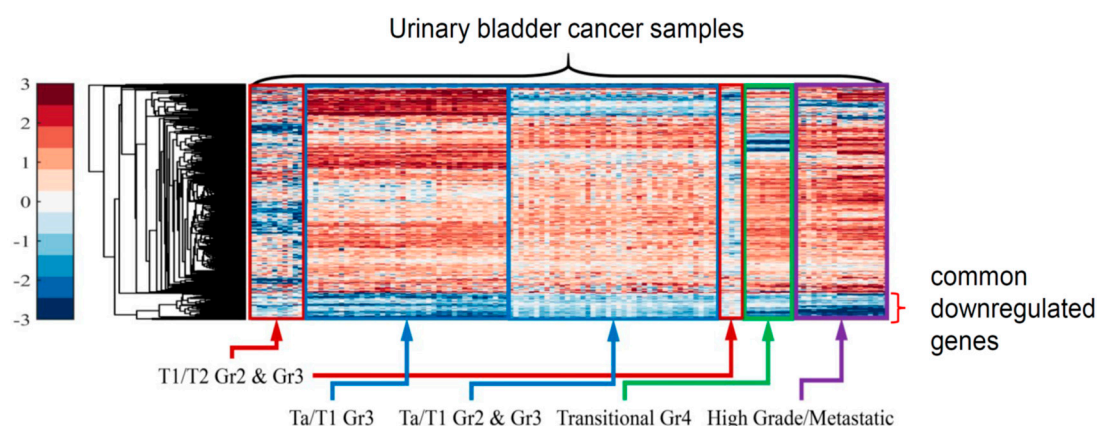


**Figure 1.** HCL of the DEGs across all urinary bladder cancer samples. The red highlight represents the common down-regulated DEGs. Arrows depict the urinary bladder cancer samples of different stage (T) and grade (Gr) that were clustered together.

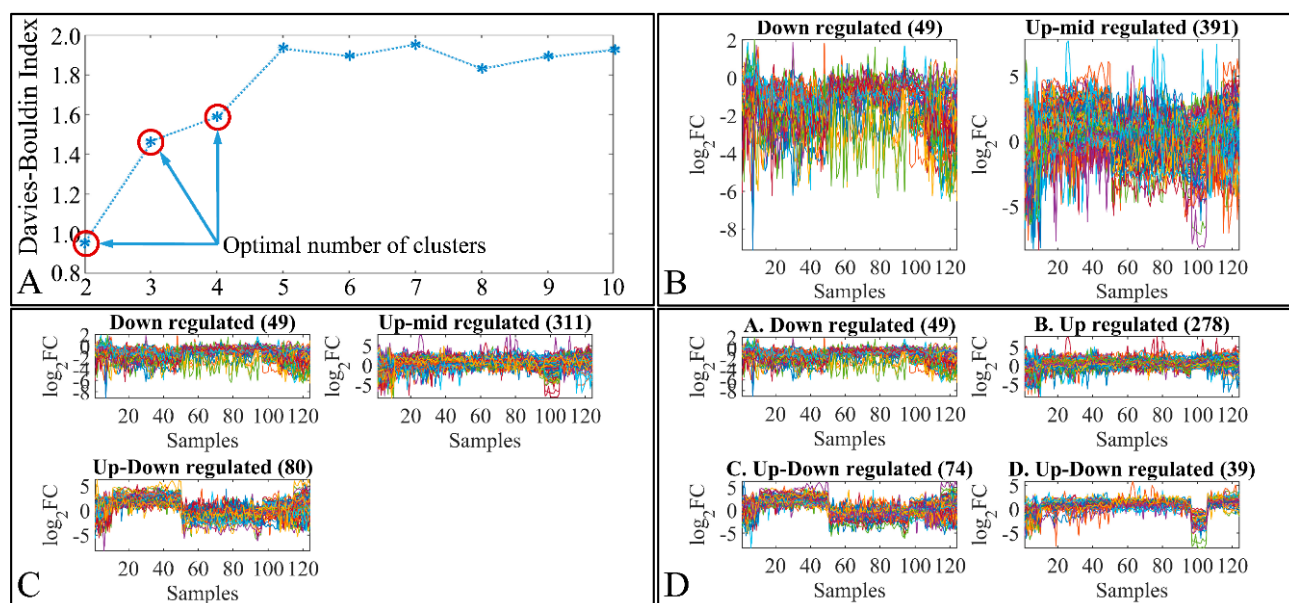


**Figure 2.** Total number of DEGs was further investigated with k-means clustering. Davies–Bouldin criterion showed that 2, 3, and 4 clusters were optimal for the present dataset (A). Genes were clustered for  $k = 2$  (B),  $k = 3$  (C) and  $k = 4$  (D), where  $k$  is the number of clusters.

### 3.2.1. Globally Down-Regulated Genes

The previous results gave us a hint that clusters A (Figure 2D) and B (Figure 2D) include genes that could be possibly up- and down-regulated, globally. Therefore, these clusters (cluster A with 49 genes and B with 278 genes, Figure 2D) were chosen for further analysis.

Additionally, we performed a k-means clustering analysis for cluster A (Figure 2D), which resulted in two sub-clusters, termed “A1” and “A2” (Figure 3A,B). This further classification was attempted in order to further separate genes based on their expressional profile. Indeed, the genes of cluster A were separated in two clusters, one of which manifested genes with lower expression (cluster A2) compared to those in cluster A1 (Figure 3B). For visualization purposes, we also performed an HCL clustering in all three clusters (Figure 4), resulting in clusters A (Figure 2D), A1 (Figure 3B), and A2 (Figure 3B). In particular, HCL manifested and visually confirmed the down-regulated pattern of k-means clusters

A (Figure 2D), A1, and A2 (Figure 3B), which are presented in Figure 4A–C. The globally down-regulated genes are also summarized in Table 1.

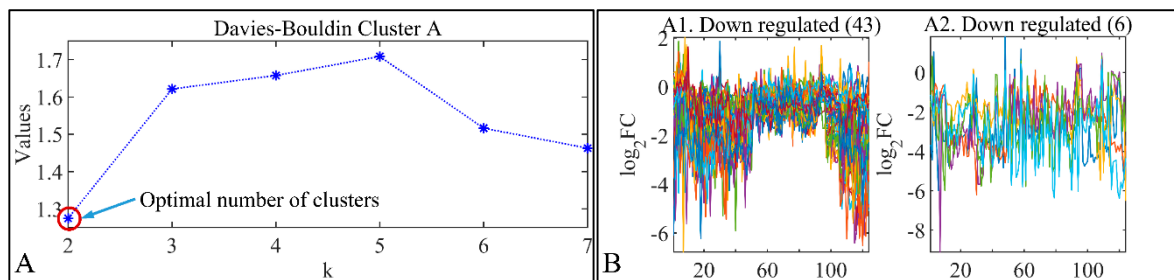


**Figure 3.** The DEGs of cluster A in Figure 2D were further investigated with k-means clustering. The Davies–Bouldin criterion revealed that 2 clusters were optimal for the present dataset (A). Genes were clustered for  $k = 2$  (B), manifesting two sub-clusters, termed A1 (43 genes) and A2 (6 genes);  $k$  is the number of clusters.

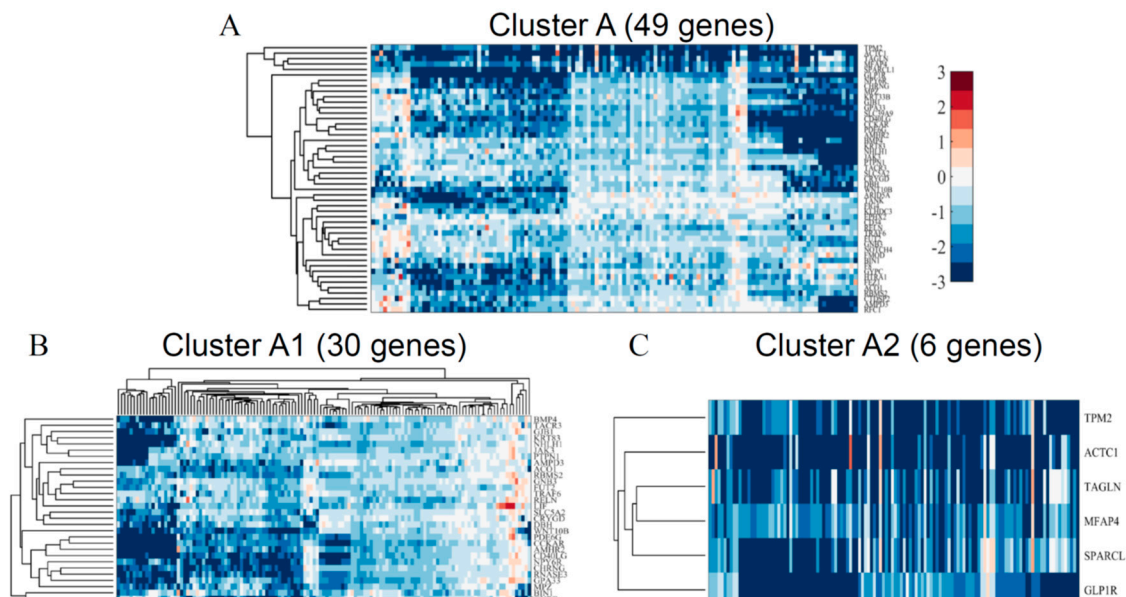


**Figure 4.** HCL of the k-means clusters presented in Figures 2D and 3B. In particular, HCL presented included cluster (A) A (Figure 2D), (B) A1 (Figure 3B) and (C) A2 (Figure 3C).

**Table 1.** Globally down-regulated genes in at least >89% of all samples.

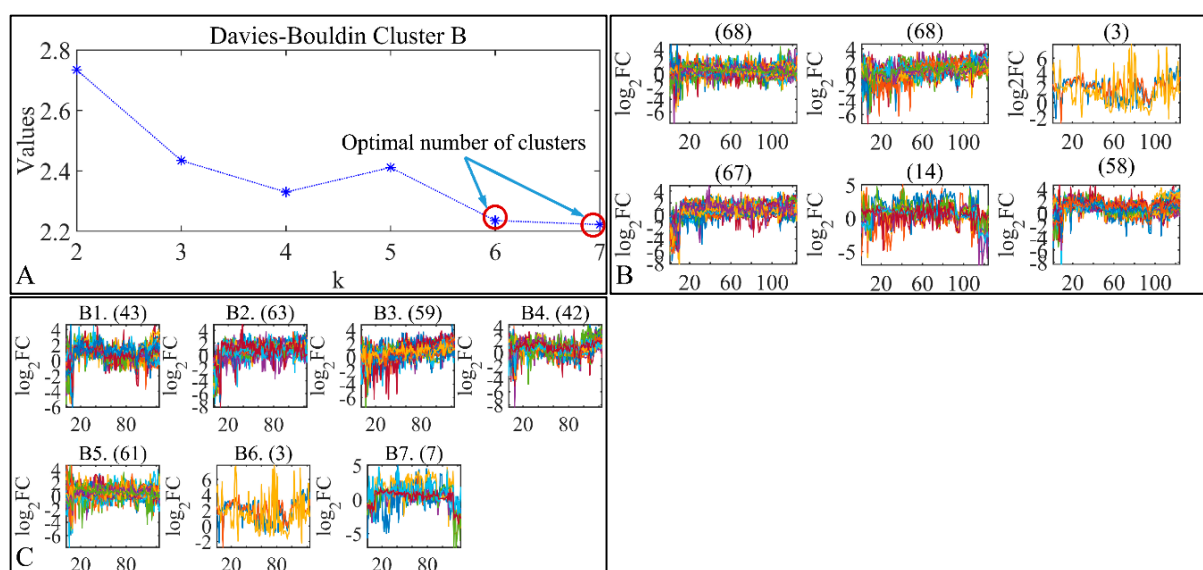
Inv.	Gene Name	Cluster	<i>n</i>	(%)
1	ACO1	A1	128	97.71%
2	CCKAR	A1	128	97.71%
3	JAK3	A1	128	97.71%
4	GLP1R	A2	127	96.95%
5	RNASE3	A1	127	96.95%
6	GJB1	A1	126	96.18%
7	KRT83	A1	126	96.18%
8	MPZ	A1	126	96.18%
9	PDE6G	A1	126	96.18%
10	TPM2	A2	126	96.18%
11	AMHR2	A1	125	95.42%
12	CD40LG	A1	125	95.42%
13	GYPC	A1	125	95.42%
14	PTPN1	A1	125	95.42%
15	SLC5A2	A1	124	94.66%
16	WNT10B	A1	124	94.66%

Table 1. Cont.

Inv.	Gene Name	Cluster	<i>n</i>	(%)
17	MFAP4	A2	123	93.89%
18	TAGLN	A2	123	93.89%
19	AMPD3	A1	122	93.13%
20	CHRNA3	A1	122	93.13%
21	GNB3	A1	122	93.13%
22	NHLH1	A1	122	93.13%
23	ACTC1	A2	121	92.37%
24	DBH	A1	121	92.37%
25	FUT2	A1	121	92.37%
26	NPY6R	A1	121	92.37%
27	TACR3	A1	121	92.37%
28	BMP4	A1	120	91.60%
29	GPA33	A1	120	91.60%
30	RBMS2	A1	120	91.60%
31	RELN	A1	120	91.60%
32	TRAF6	A1	120	91.60%
33	BIN1	A1	119	90.84%
34	CRYGD	A1	119	90.84%
35	LIF	A1	119	90.84%
36	SPARCL1	A2	117	89.31%

### 3.2.2. Globally Up-Regulated Genes

Similarly, we followed this procedure for the up-regulated genes. In particular, the optimal number of clusters was calculated to be 6 and 7 (Figure 5A), presented as k-means clusters (Figure 5B,C). The clusters B1, B2, B6, and B7, manifested possibly globally up-regulated genes (Figure 5C), whose HCLs are presented in Figure 6. We identified 30 genes, which were globally up-regulated in >80% of all tumor samples (Figure 6). The identified genes included YES1, PMM1, IRF3, ARL6IP1, CYTH2, LASP1, PSMD2, PSMD7, DDOST, NDUFB2, RALY, ADRM1 (Figure 6B), HMGA1, RPN1, TXN, TYK2, UNG, EBNA1BP2, IGF2R, PCNA, PTMA, SNRPA, USP7, and VDAC1 (Figure 6C), CDC20, KRT14, APOBEC3B (Figure 6D), YWHAB, STMN1, and MCM5 (Figure 6E). The globally up-regulated genes are summarized in Table 2.



**Figure 5.** The DEGs of cluster B in Figure 4D, were further investigated with k-means clustering. Davies–Bouldin criterion showed that 2 clusters were optimal for the present dataset (A). Genes were clustered for  $k = 6$  (B) and  $k = 7$  (C), manifesting six clusters (B) and seven clusters (B1–B7) (C) respectively, where  $k$  is the number of clusters.

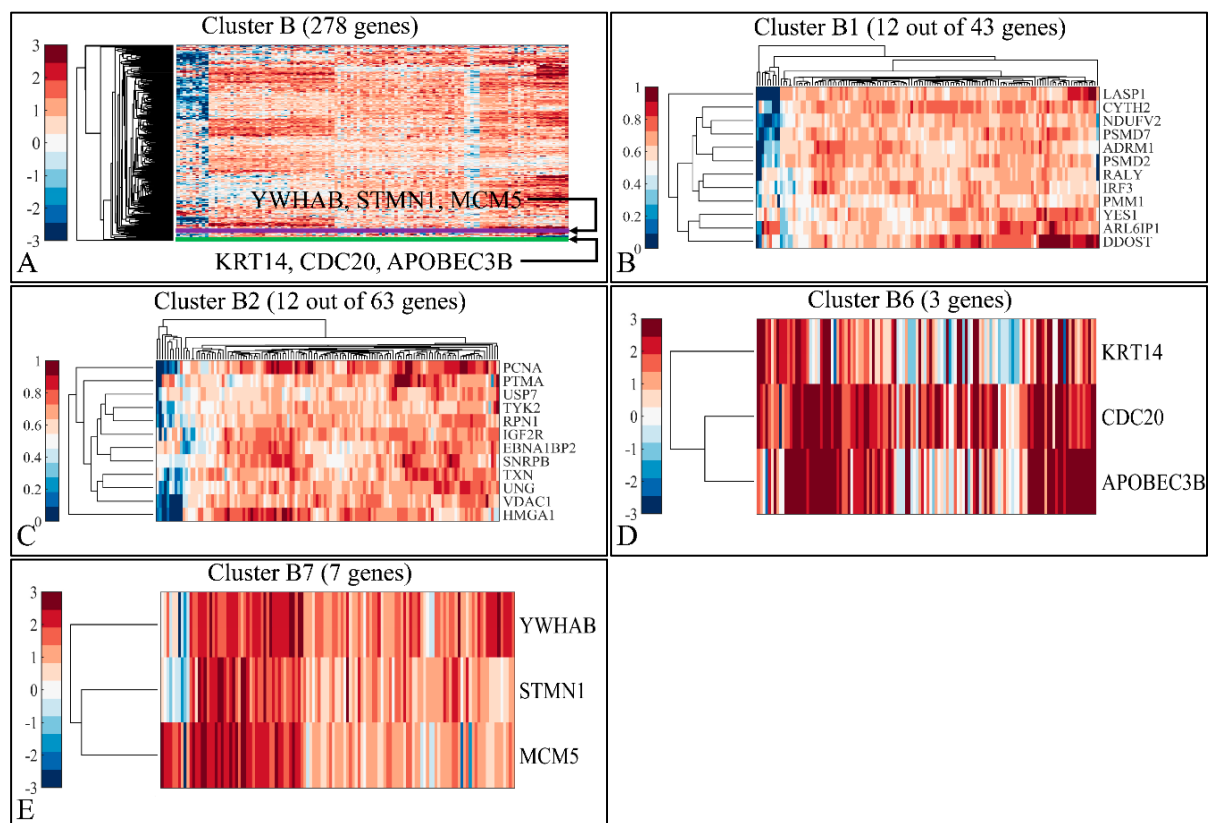


**Figure 6.** HCL of the k-means clusters presented in Figure 2D (cluster B) (A) and Figure 5C (cluster B1, cluster B2, cluster B6, and cluster B7) (B–E).

**Table 2.** Globally up-regulated genes in  $\geq 80\%$  of all tumor samples.

Inv.	Gene Name	Cluster	<i>n</i>	(%)
1	YES1	B1	125	95.42%
2	PMM1	B1	123	93.89%
3	CDC20	B6	123	93.89%
4	IRF3	B1	122	93.13%
5	MCM5	B7	122	93.13%
6	ARL6IP1	B1	121	92.37%
7	CYTH2	B1	121	92.37%
8	LASP1	B1	121	92.37%
9	PSMD2	B1	121	92.37%
10	PSMD7	B1	121	92.37%
11	DDOST	B1	120	91.60%
12	NDUFV2	B1	120	91.60%
13	RALY	B1	120	91.60%
14	STMN1	B7	120	91.60%
15	ADRM1	B1	119	90.84%
16	HMGA1	B2	119	90.84%
17	RPN1	B2	119	90.84%
18	TXN	B2	119	90.84%
19	TYK2	B2	119	90.84%
20	UNG	B2	119	90.84%
21	EBNA1BP2	B2	118	90.08%
22	IGF2R	B2	118	90.08%
23	PCNA	B2	118	90.08%
24	PTMA	B2	118	90.08%
25	SNRPB	B2	118	90.08%
26	USP7	B2	118	90.08%

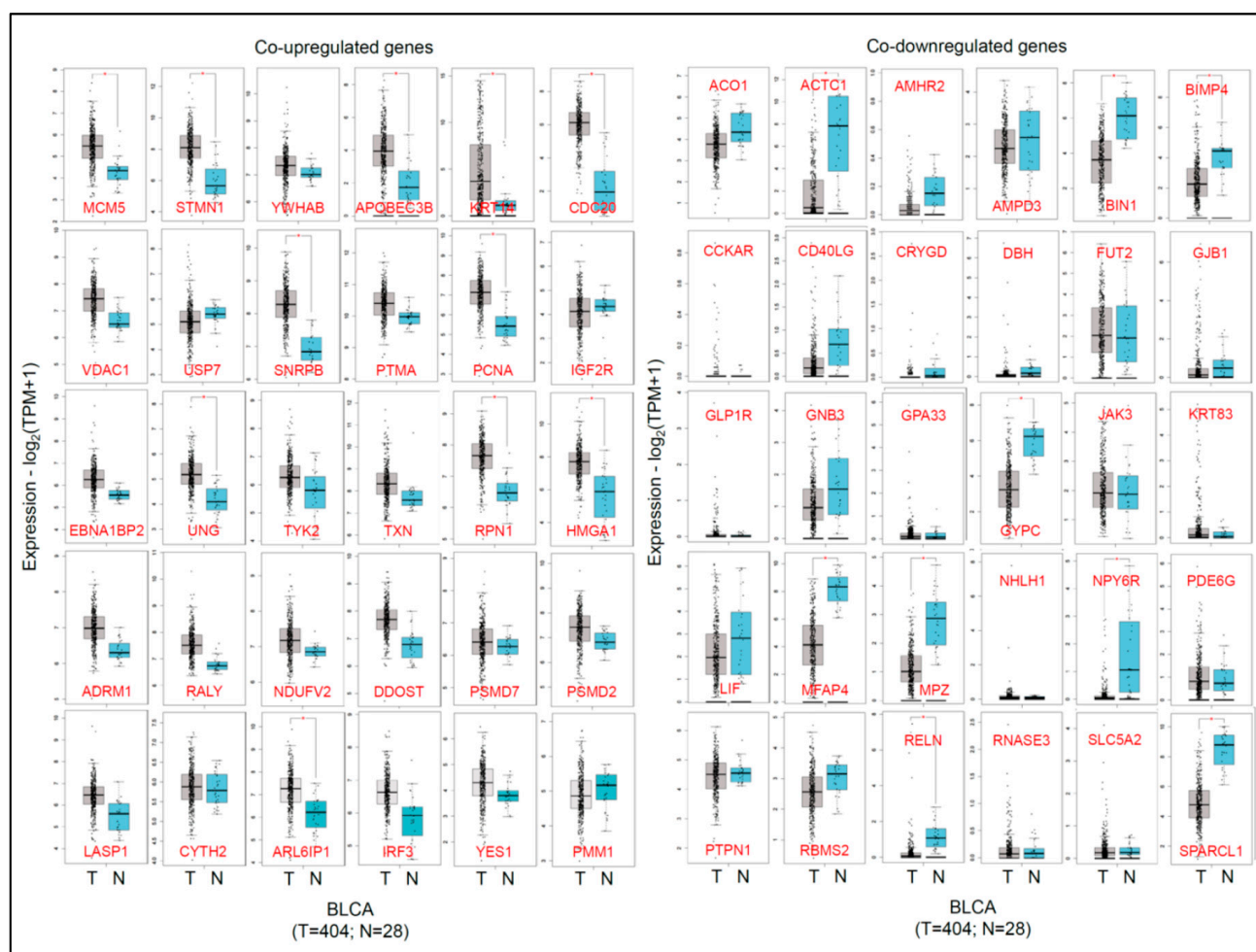


Table 2. Cont.

Inv.	Gene Name	Cluster	n	(%)
27	VDAC1	B2	118	90.08%
28	YWHAB	B7	118	90.08%
29	APOBEC3B	B6	106	80.92%
30	KRT14	B6	96	73.28%

### 3.2.3. Cohort Validation

We validated 25 upregulated and 19 downregulated genes (83.33% and 63.33% accuracy, respectively) out of the top 30 DEGs in bladder cancer, compared to a mixed sample of normal urothelia extracted from the TCGA-BLCA and GTEx projects. The genes MCM5, STMN1, APOBEC3B, KRT14, CDC20, SNRPB, PCNA, UNG, RPN1, HMGA1a, and ARL6IP1 exhibited the highest upregulation across all urinary bladder cancer samples ( $\log_2FC > 1$ ,  $p < 0.001$ ); whereas, ACTC1, BIN1, BIMP4, GYPC, MFAP4, MPZ, NPY6R, RELN and SPARCL1, the highest downregulation ( $\log_2FC < 1$ ,  $p < 0.001$ ) (Figure 7).



**Figure 7.** Validation of the top 30 upregulated and top 30 downregulated genes in urinary bladder cancer, using the TCGA-BLCA and GTEx datasets. The red stars (\*) denote statistically significant differences in gene expression (for the top downregulated genes,  $\log_2FC < 1$  and  $p < 0.001$ ; for the top upregulated genes,  $\log_2FC > 1$  and  $p < 0.001$ ).

### 3.3. Functional Annotation of the DEGs

Our analysis manifested globally up- and down-regulated genes that were further analyzed for their functional annotation.

### 3.3.1. Functional Annotation of Globally Down-Regulated Genes

The down-regulated genes did not manifest any significant gene ontological function; yet they participated in “Pathways in Cancer” and “Basal Cell Carcinoma”, along with “signaling pathways regulating pluripotency of stem cells” (Figure 8A). In addition, we queried for drug annotations related to these genes and found that they are related to Vardenafil, Pyridone 6, Manganese, Disulfiram, Cholecystokinin, Tofacitinib, Pranlukast, 3-isobutyl-1-methyl-7H-xanthine, Ertugliflozin, and Semaglutide (Figure 8B). Among the drugs with the highest enrichment ration, Vardenafil and Disulfiram, an erectile dysfunction drug and a proteasome inhibitor, respectively, were of particular interest. Ertugliflozin and Semaglutide are also two drugs of potential interest since both constitute glucose resorption factors.

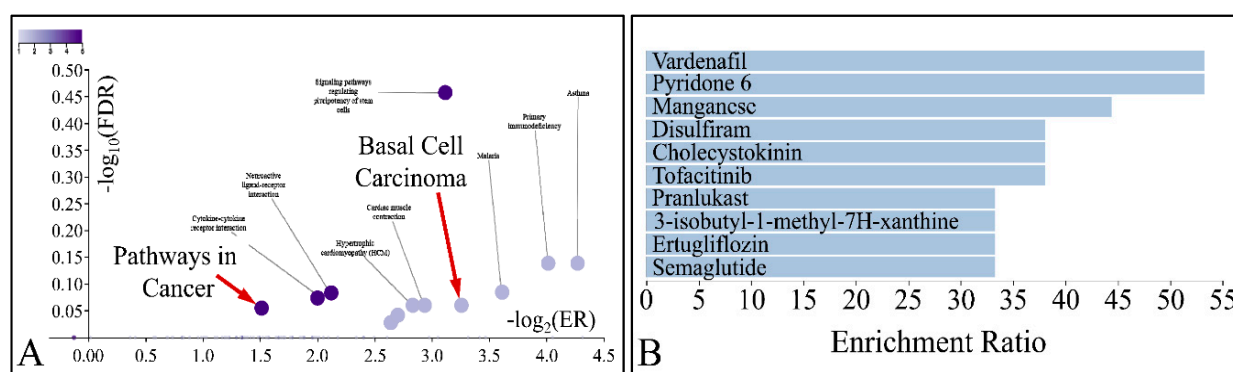


**Figure 8.** Pathway annotation (A) and drug annotation (B) of the globally down-regulated DEGs (Legend: ER: enrichment ratio, FDR: false discovery ratio).

### 3.3.2. Functional Annotation of the Globally Up-Regulated Genes

Similarly, we assessed the functional annotation of the globally up-regulated genes across all UBC samples and found that the DEGs participate in protein binding, in terms of their molecular function. In addition, they are related to the proteasome (Figure 9A, Table 3). These findings were confirmed by the pathway annotation analysis, where the DEGs manifested participation in the proteasome and cell cycle pathways, but also in base excision repair, DNA replication, N-glycan biosynthesis, and cell cycle and Epstein - Barr virus infection, among others (Figure 9B). Finally, the investigation of drug annotation showed that DEGs were related to Pyridone 6, 1D-myo-inositol 1,4,5-triphosphate, Tofacitinib, Inositol 1,3,4,5-tetrakisphosphate, S,S-2-(Hydroxyethyl) Thiocysteine, Formic Acid, Liothyronine, Phenethyl Isothiocyanate, Dasatinib and Medical Cannabis (Figure 9C).

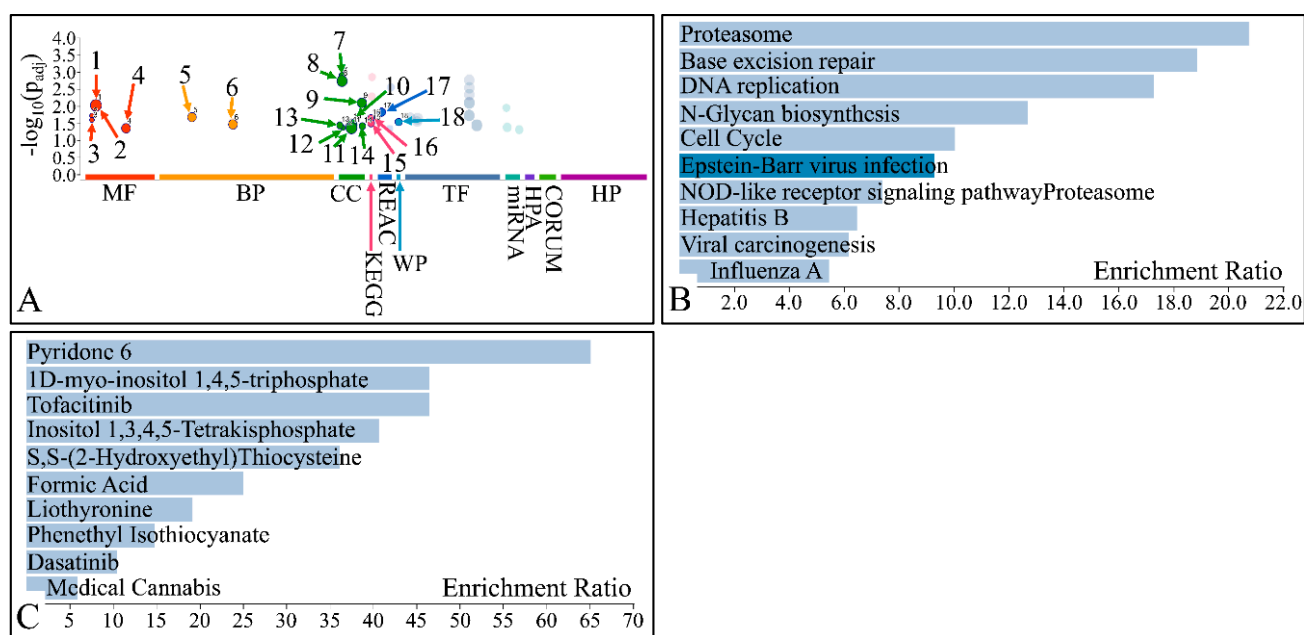


**Figure 9.** Functional annotation of the globally up-regulated DEGs in UBC. The annotation analysis includes gene ontology (GO) enrichment (**A**), pathway analysis (**B**), and drug annotation (**C**) (Legend: MF: molecular function, BP: biological process, CC: cellular component, KEGG: KEGG pathway database, REAC: reactome pathway database, WP: Wikipathways, TF: transcription factor-binding motifs, MIRNA: MiRNA targets, HPA: he Human Protein Atlas, CORUM: The Comprehensive Resource of Mammalian Protein Complexes, HP: human phenotype ontology).

**Table 3.** Gene Ontology annotations of the globally up-regulated genes, as depicted in Figure 8A.

ID	Source	Term	Term ID	$P_{adj}$	Genes
1	GO:MF	protein binding	GO:0005515	0.009515	YES1,PMM1,CDC20,IRF3,MCM5,ARL6IP1,CYTH2,LASP1,PSMD2,PSMD7,DDOST,NDUFV2,RALY,STMN1,ADRM1,HMGA1,RPN1,TXN, TYK2,UNG,EBNA1BP2,IGF2R,PCNA,PTMA,SNRBP,USP7,VDAC1, YWHAB,APOBEC3B,KRT14
2	GO:MF	dolichyl-diphosphooligosaccharide-protein glycotransferase activity	GO:0004579	0.019061	DDOST,RPN1
3	GO:MF	oligosaccharyl transferase activity	GO:0004576	0.025388	DDOST,RPN1
4	GO:MF	protein-containing complex binding	GO:0044877	0.044508	CDC20,LASP1,ADRM1,UNG,PCNA,SNRBP,VDAC1,YWHAB,KRT14
5	GO:BP	viral process	GO:0016032	0.021014	IRF3,HMGA1,UNG,IGF2R,PCNA,USP7,VDAC1,YWHAB,APOBEC3B
	GO:BP	interspecies interaction between organisms	GO:0044419	0.031201	IRF3,PSMD2,PSMD7,STMN1,HMGA1,TYK2,UNG,IGF2R,PCNA,USP7, VDAC1,YWHAB,APOBEC3B
6	GO:BP	symbiotic process	GO:0044403	0.034472	IRF3,HMGA1,UNG,IGF2R,PCNA,USP7,VDAC1,YWHAB,APOBEC3B
7	GO:CC	proteasome regulatory particle	GO:0005838	0.001241	PSMD2,PSMD7,ADRM1
8	GO:CC	cytosol	GO:0005829	0.001839	YES1,PMM1,CDC20,IRF3,MCM5,ARL6IP1,CYTH2,PSMD2,PSMD7, STMN1,ADRM1,HMGA1,RPN1,TXN, TYK2,PTMA,SNRBP,USP7, YWHAB,KRT14
	GO:CC	proteasome accessory complex	GO:0022624	0.001847	PSMD2,PSMD7,ADRM1
9	GO:CC	catalytic complex	GO:1902494	0.007993	CDC20,PSMD2,PSMD7,DDOST,NDUFV2,RALY,ADRM1,RPN1, PCNA,SNRBP
10	GO:CC	intracellular organelle	GO:0043229	0.035435	YES1,CDC20,IRF3,MCM5,ARL6IP1,CYTH2,LASP1,PSMD2,PSMD7, DDOST,NDUFV2,RALY,STMN1,ADRM1,HMGA1,RPN1,TXN, TYK2, UNG,EBNA1BP2,IGF2R,PCNA,PTMA,SNRBP,USP7,VDAC1,YWHAB, APOBEC3B,KRT14
11	GO:CC	proteasome complex	GO:0000502	0.036772	PSMD2,PSMD7,ADRM1
12	GO:CC	endopeptidase complex	GO:1905369	0.038428	PSMD2,PSMD7,ADRM1
13	GO:CC	oligosaccharyltransferase complex	GO:0008250	0.042715	DDOST,RPN1

Table 3. Cont.

ID	Source	Term	Term ID	$P_{adj}$	Genes
14	GO:CC	intracellular membrane-bounded organelle	GO:0043231	0.043905	YES1,CDC20,IRF3,MCM5,ARL6IP1,CYTH2,PSMD2,PSMD7,DDOST,NDUFV2,RALY,ADRM1,HMGA1,RPN1,TXN,TYK2,UNG,EBNA1BP2,IGF2R,PCNA,PTMA,SNRPB,USP7,VDAC1,YWHAB,APOBEC3B,KRT14
15	KEGG	Proteasome	KEGG:03050	0.022187	PSMD2,PSMD7,ADRM1
16	KEGG	Cell cycle	KEGG:04110	0.031652	CDC20,MCM5,PCNA,YWHAB
17	REAC	Ub-specific processing proteases	REAC:R-HSA-5689880	0.002821	CDC20,PSMD2,PSMD7,ADRM1,USP7,VDAC1
18	WP	Cell Cycle	WP:WP179	0.029044	CDC20,MCM5,PCNA,YWHAB



#### 4. Discussion

In the present work, we investigated for the first time the presence of globally up- and down-regulated genes in UBC. Microarray experiments consist of a series of experimental and analysis steps, among which, the clustering of the data at hand is of major importance. Clustering is one of the most important functions in data analysis [32]. Some of the main tasks that clustering algorithms are called upon to solve, is gaining insight into data, classifying, and compressing them [33]. Clustering approaches aim to extract sets of genes with similar expression profiles across all samples, or in a subset of them [34]. This is mainly accomplished by using 2D matrices of the form *Genes*  $\times$  *Samples*, on which appropriate clustering algorithms are applied. The k-means or bi-clustering techniques are good examples of such algorithms [35–41]. There are also numerous proposals in the literature regarding the analysis of time-series microarray data. In such cases, a series of cDNA microarray experiments are performed in different time points, and then clustering techniques on a 3D matrix of the form *Time*  $\times$  *Genes*  $\times$  *Samples* are applied [34,42–51].

In the present study, our main approach was to use different clustering methods. We focused, however, on the k-means algorithm, since it is very efficient for grouping expression patterns. It is also relatively easy to implement, it can be used for large datasets, and has the significant advantage of calculating data trends by estimating the centroids [52–55]. For small cluster numbers (*k* values), it converges very quickly to the local optimal, allowing a sufficient number of initializations to be used [56–60]. An important methodological parameter is the number of clusters. It is considered a difficult task since it influences the final outcome, i.e., which genes will be clustered together. A frequent approach is to test several appropriate values of *k*, in order to find patterns in expression data. In the present work, the Davies–Bouldin criterion helped in this direction, which successfully gave the optimal *k* clusters [61].

Unlike k-means, hierarchical clustering algorithms do not offer user-defined configuration options. The only option that can be made is to calculate the distance between clusters. In this case, we chose to use the UPGMA method, which defines the distance between two blocks as the average distance between all elements. Therefore, we used UPGMA in combination with k-means clustering. It has been previously shown that HCL groupings based on k-means clusters, perform well [18]. A major disadvantage of the HCL algorithm is that it requires large amounts of memory in order to store the “Dissimilarity Matrix”, making it difficult to implement when the number of data is large.

This mode of analysis led us to the identification of 36 globally down-regulated and 30 globally up-regulated DEGs. The co-up-regulated genes could pose a more interesting therapeutic target since gene inhibition is probably easier, compared to the induction of gene expression. The genes YES1 and PMM1 were the ones with the highest percentage of up-regulation among all tumor samples. To our knowledge, there is no known relation between YES1 or PMM1 and UBC. In addition, no known relations were found for the role of *IRF3*, *ARL6IP1*, *CYTH2*, *PSMD2*, *PSMD7*, *NDUFB2*, *RALY*, *ADRM1*, *RPN1*, *TYK2*, *UNG*, *EBNA1BP2*, *SNRPB*, and *VDAC1* in UBC; therefore, these genes could be the topic of future studies.

Among the co-upregulated genes, we found CDC20, which was also previously reported to be deregulated in urinary bladder cancer [20]. The rest genes were not previously identified as co-DEGs in UBC. CDC20 encodes the cell-division cycle protein 20, a regulatory protein that interacts with several other proteins at multiple points in the cell cycle [62]. It has been observed to be highly expressed in high-grade cancers and is associated with a poor prognosis in breast, pancreatic, bladder, and lung cancers [62]. In previous studies, specifically conducted on bladder cancer, CDC20 was presented as a biomarker that associates with poor prognosis [63,64]. Another report showed that in breast cancer, CDC20 limits the activity of the tumor suppressor *SMAR1* [62], while there is evidence that the tumor suppressor *TP53* inhibits the growth of cancer cells through indirect regulation of CDC20 [65]. In all, CDC20 is often cited in the literature as a “potentially innovative therapeutic target” for cancer treatment [65,66].

The *MCM5* (Minichromosome Maintenance Deficient 5) gene, also known as CDC46, encodes the DNA replication licensing factor protein MCM5, which is implicated in initiating DNA replication. The MCM5 protein is up-regulated during the transition from the G<sub>0</sub> phase to the G<sub>1</sub>/S phase of the cell cycle and can be actively involved in its regulation. Previous studies have shown that the MCM5 protein is a very reliable biomarker for the diagnosis and prognosis of bladder cancer. Completely differentiated cells of the healthy epithelium do not express this gene, yet cancer cells that show intense cell division strongly express *MCM5*, making its protein detectable in urine [67]. Among several FDA-approved diagnostic tests for the early detection of bladder cancer (cystoscopy, urine cytology, ImmunoCyt, and UroVysion), as well as for the detection of the biomarkers NMP22 (Nuclear matrix protein 22), BTA (bladder tumor antigen), MCM5 is a very reliable biomarker, regardless of the cancer type, with >70% sensitivity and >95% Negative Predictive Value (NPV) [67–70].

Interestingly, *LASP1* has been previously reported in the literature as a potential diagnostic marker of UBC [71–73]. The above-mentioned reports are in good agreement with our findings.

In another report, the *DDOST* gene was found to be hypo-methylated and over-expressed in the majority of UBC samples. In particular, *DDOST* was in the core of the built protein-protein network in these tumors [74]. Although this was a single report on *DDOST* in UBC, it is also in agreement with our findings.

*SMTN1* is another interesting gene that we revealed. This gene encodes the Stathmin protein, which is also known as oncoprotein 18. This is very important for the regulation of the cytoskeleton, which is involved in many cellular processes, such as cytoplasmic organization, cell division and cell division [75]. In a recent report, it was shown that Stathmin is highly expressed in a wide range of cancers [76], including those of the lung, esophagus, breast, cervix, bladder urothelial carcinoma, and glioblastoma. In addition, the same study concluded that targeting this gene reduces cell proliferation, cell motility, and increases the apoptosis of neoplastic tumors. Specifically in UBC, it has been reported that Stathmin was found: (a) to be low or even not-expressed in the healthy urothelium, (b) to correlate between high protein expression and tumor high stage and degree, (c) to be expressed in the majority of metastatic cancers. These studies are in agreement with our report, declaring *STMN1* as a potential therapeutic target of great potential [77].

*HMGA1* is another interesting up-regulated gene, connected to the tumor's progression and therapy resistance [78–82]. These reports are in accordance with our findings since *HMGA1* was also up-regulated in >90% of tumors in our study, indicating that they indeed manifest similar genotypic profiles.

Another interesting report showed that the *TXN* gene is probably a direct target of luteolin, which inhibits tumor proliferation through the rapamycin pathway [83]. On the other hand, *PTMA* [84], *IGFR2* [85], and *YWHAB* [86] are reported in the literature as three genes whose down-regulation is related to poor prognosis, cell proliferation enhancement, and anti-apoptosis, and are thus suspected to act as tumor suppressors. This is in contrast to our findings, where these genes were globally up-regulated. Our finding that *USP7* is globally up-regulated, is in line with two previous reports, which indicated that *USP7* inhibition is a potential therapy for UBC [87,88].

In addition, *PCNA* was found to be globally up-regulated in UBC. This is one of the best-studied genes in this tumor type. It is a well-known proliferation marker, related to tumor progression and anti-apoptosis; thus, it acts as an oncogene. The majority of studies agree that *PCNA* over-expression is related to tumor progression and survival [89–93]. In addition, *PCNA* inhibition was directly connected to UBC therapy, where it has been shown to function as an anti-tumor agent [90,94–96]. These findings are in good agreement with our results, in which *PCNA* was globally up-regulated in UBC.

The accumulation of various mutations may be due to exogenous or endogenous factors and is closely related to the development of carcinogenesis. There is increasing evidence that *APOBEC3B* is a broadly mutagenic agent in multiple tumor types [97]. It also

shows increased expression, affecting the ontogenesis and progression of various cancers, including those of the neck, breast, lung, head, and bladder. The APOBEC3B gene functions as a cytidine to uridine (C-to-U) editor, and it is heavily implicated in innate and adaptive immunity with important roles in antibody diversification and antiviral response [98]. It also plays an important role in the functions of the immune system, introducing mutations to the viral genomes [99–102]. This was confirmed by our functional annotation analysis showing that the identified DEGs, manifested antiviral-related functions. It is reasonable to assume that APOBEC3B inhibitors can prevent the accumulation of mutations in certain cancers, making it a promising therapeutic target. APOBEC3B is often reported in the literature with the terms “mutagen” and “tumor mutator” [103–107].

Another interesting gene that our analysis revealed is *KRT14*. This encodes the protein keratin 14, which is a type I keratin being part of the cell skeleton of epithelial cells. The bladder epithelium, also known as the urothelium, is made up of 3 different cell types. The first layer, or superficial layer, coats the inner surface of the bladder and is made up of “umbrella cells”. The next layers consist of the intermediate and the basal layers, which come in contact with the skin. In several studies performed in mice, it has been shown that the cells of the basal layer, expressing *KRT14*, are responsible for the regeneration of urothelium in the event of injury, and are cells responsible for the oncogenesis in the bladder [108,109]. According to a previous study, *KRT14* expression in bladder cancer is strongly associated with poor prognosis for survival, regardless of other clinical variables such as the stage of cancer, age, or sex [110]. Thus, it has been suggested that *KRT14* is a possible prognostic biomarker for distinguishing between high and low-risk patients.

Finally, we observed that the globally up-regulated genes were mostly involved in molecular functions related to the proteasome and protein-protein binding, while the annotated pathways, included viral carcinogenesis and proteasomal functions. On the other hand, the globally down-regulated genes were found to participate in different pathways in cancer, as well as basal cell carcinoma pathways.

## 5. Conclusions

In the present work, we identified 36 down-regulated and 30 up-regulated genes, across different subtypes of urinary bladder cancer stemming from various microarray datasets. Importantly, we validated most of these DEGs in an independent dataset from the TCGA, where gene expression was assessed using RNAseq. To the best of our knowledge, there is no previous work identifying common gene expression patterns in UBC. Our study identified genes that are in agreement with previous studies regarding their implication in the disease, as well as working as predictors of tumor prognosis, progression, and therapy. The methodology of finding co-deregulated patterns of gene expression across different studies could constitute a basis for the discovery of tumor biomarkers for therapy, prognosis, and diagnosis.

**Supplementary Materials:** The following are available online at <https://www.mdpi.com/2076-3417/11/4/1785/s1>, Figure S1: Calculated False Discovery Rate (FDR) for the common gene dataset (Legend:  $\hat{\pi}_0 = \frac{m_0}{m}$ , where,  $m_0$  and  $m$  are the number of true null hypotheses and the total number hypotheses tested respectively,  $p$ -value is the obtained  $p$ -value for each gene,  $q$ -value is the respective  $q$ -value for each gene,  $\lambda$  is the threshold after which the proportion of truly null features equals the number of  $p$ -values greater than  $\lambda$  divided by  $m(1 - \lambda)$ ). Figure S2: Schematic representation of  $p$ -values vs.  $q$ -values (A), the  $q$ -values vs. the expected number of significant genes (B) and the number of expected significant genes vs. the number of false positives (C). Table S1: Summary of the microarray experiments (data series) used in the present study (Legend: UBC: Urinary Bladder Cancer, the indication GrX implies a UBC of unknown grade). Table S2: The estimated parameters of the FDR calculations.

**Author Contributions:** G.I.L., Conceptualization, methodology, software, validation, formal analysis, investigation, data curation, writing-original draft preparation, visualization, resources, supervision; K.V., Methodology, software, validation, formal analysis, data curation; D.K., Supervision, project ad-

ministration; A.Z., Conceptualization, methodology, validation, investigation, data curation, writing—original draft preparation, writing—review and editing, visualization, funding acquisition. All authors have read and agreed to the published version of the manuscript.

**Funding:** This research received no external funding.

**Conflicts of Interest:** The authors declare no conflict of interest.

## References

1. Bilski, K.; Dobruch, J.; Kozikowski, M.; Skrzypczyk, M.A.; Oszczudlowski, M.; Ostrowski, J. Urobiome in gender-related diversities of bladder cancer. *Int. J. Mol. Sci.* **2020**, *21*, 4488. [\[CrossRef\]](#) [\[PubMed\]](#)
2. Antoni, S.; Ferlay, J.; Soerjomataram, I.; Znaor, A.; Jemal, A.; Bray, F. Bladder cancer incidence and mortality: A global overview and recent trends. *Eur. Urol.* **2017**, *71*, 96–108. [\[CrossRef\]](#) [\[PubMed\]](#)
3. Center, M.M.; Jemal, A.; Lortet-Tieulent, J.; Ward, E.; Ferlay, J.; Brawley, O.; Bray, F. International variation in prostate cancer incidence and mortality rates. *Eur. Urol.* **2012**, *61*, 1079–1092. [\[CrossRef\]](#) [\[PubMed\]](#)
4. Ferlay, J.; Soerjomataram, I.; Dikshit, R.; Eser, S.; Mathers, C.; Rebelo, M.; Parkin, D.M.; Forman, D.; Bray, F. Cancer incidence and mortality worldwide: Sources, methods and major patterns in globocan 2012. *Int. J. Cancer* **2015**, *136*, E359–E386. [\[CrossRef\]](#) [\[PubMed\]](#)
5. Fidler, M.M.; Gupta, S.; Soerjomataram, I.; Ferlay, J.; Steliarova-Foucher, E.; Bray, F. Cancer incidence and mortality among young adults aged 20–39 years worldwide in 2012: A population-based study. *Lancet. Oncol.* **2017**, *18*, 1579–1589. [\[CrossRef\]](#)
6. Babjuk, M.; Bohle, A.; Burger, M.; Capoun, O.; Cohen, D.; Comperat, E.M.; Hernandez, V.; Kaasinen, E.; Palou, J.; Roupert, M.; et al. Eau guidelines on non-muscle-invasive urothelial carcinoma of the bladder: Update 2016. *Eur. Urol.* **2017**, *71*, 447–461. [\[CrossRef\]](#)
7. Dyrskjot, L.; Kruhoffer, M.; Thykjaer, T.; Marcussen, N.; Jensen, J.L.; Moller, K.; Orntoft, T.F. Gene expression in the urinary bladder: A common carcinoma in situ gene expression signature exists disregarding histopathological classification. *Cancer Res.* **2004**, *64*, 4040–4048. [\[CrossRef\]](#)
8. Kawahara, T.; Kojima, T.; Kandori, S.; Kurobe, M.; Yoshino, T.; Kimura, T.; Nagumo, Y.; Ishituka, R.; Mitsuzuka, K.; Narita, S.; et al. Tp53 codon 72 polymorphism is associated with fgfr3 and ras mutation in non-muscle-invasive bladder cancer. *PLoS ONE* **2019**, *14*, e0220173. [\[CrossRef\]](#)
9. Boulalas, I.; Zaravinos, A.; Karyotis, I.; Delakas, D.; Spandidos, D.A. Activation of ras family genes in urothelial carcinoma. *J. Urol.* **2009**, *181*, 2312–2319. [\[CrossRef\]](#)
10. Elwy, A.E.; Elsaba, T.M.; Elzahr, A.R.A.; Nassar, M.I. Prognostic value of c-myc immunohistochemical expression in muscle invasive urothelial carcinoma of the urinary bladder: A retrospective study. *Asian Pac. J. Cancer Prev. Apjcp* **2019**, *20*, 3735–3746. [\[CrossRef\]](#)
11. Kim, D.; Kim, J.M.; Kim, J.S.; Kim, S.; Kim, K.H. Differential expression and clinicopathological significance of her2, indoleamine 2,3-dioxygenase and pd-l1 in urothelial carcinoma of the bladder. *J. Clin. Med.* **2020**, *9*, 1265. [\[CrossRef\]](#) [\[PubMed\]](#)
12. Lipunova, N.; Wesseli, A.; Cheng, K.K.; van Schooten, F.J.; Cazier, J.B.; Bryan, R.T.; Zeegers, M.P. Systematic review: Genetic associations for prognostic factors of urinary bladder cancer. *Biomark. Cancer* **2019**, *11*, 1–9. [\[CrossRef\]](#) [\[PubMed\]](#)
13. Lima, A.P.B.; Almeida, T.C.; Barros, T.M.B.; Rocha, L.C.M.; Garcia, C.C.M.; da Silva, G.N. Toxicogenetic and antiproliferative effects of chrysin in urinary bladder cancer cells. *Mutagenesis* **2020**. [\[CrossRef\]](#) [\[PubMed\]](#)
14. Zeng, H.; Zhou, Q.; Wang, Z.; Zhang, H.; Liu, Z.; Huang, Q.; Wang, J.; Chang, Y.; Bai, Q.; Xia, Y.; et al. Stromal lag-3(+) cells infiltration defines poor prognosis subtype muscle-invasive bladder cancer with immunoevasive contexture. *J. Immunother. Cancer* **2020**, *8*, e000651. [\[CrossRef\]](#)
15. De Martino, M.; Zhuang, D.; Klatte, T.; Rieken, M.; Roupert, M.; Xylinas, E.; Clozel, T.; Krzywinski, M.; Elemento, O.; Shariat, S.F. Impact of erbb2 mutations on in vitro sensitivity of bladder cancer to lapatinib. *Cancer Biol. Ther.* **2014**, *15*, 1239–1247. [\[CrossRef\]](#)
16. Erben, P.; Wezel, F.; Wirtz, R.; Martini, T.; Stein, D.; Weis, C.A.; Hartmann, A.; Bolenz, C. Role of the human erbb family receptors in urothelial carcinoma of the bladder: Mrna expression status and prognostic relevance. *Aktuelle Urol.* **2017**, *48*, 356–362.
17. Gunes, S.; Sullu, Y.; Yegin, Z.; Buyukalpelli, R.; Tomak, L.; Bagci, H. Erbb receptor tyrosine kinase family expression levels in urothelial bladder carcinoma. *Pathol. Res. Pract.* **2013**, *209*, 99–104. [\[CrossRef\]](#)
18. Quackenbush, J. Computational approaches to analysis of DNA microarray data. *Yearb. Med. Inform.* **2006**, 91–103.
19. Tsai, C.A.; Chen, C.H.; Lee, T.C.; Ho, I.C.; Yang, U.C.; Chen, J.J. Gene selection for sample classifications in microarray experiments. *DNA Cell Biol.* **2004**, *23*, 607–614. [\[CrossRef\]](#)
20. Zaravinos, A.; Lambrou, G.I.; Boulalas, I.; Delakas, D.; Spandidos, D.A. Identification of common differentially expressed genes in urinary bladder cancer. *PLoS ONE* **2011**, *6*, e18135. [\[CrossRef\]](#)
21. Zaravinos, A.; Lambrou, G.I.; Volanis, D.; Delakas, D.; Spandidos, D.A. Spotlight on differentially expressed genes in urinary bladder cancer. *PLoS ONE* **2011**, *6*, e18255. [\[CrossRef\]](#)
22. Ramasamy, A.; Mondry, A.; Holmes, C.C.; Altman, D.G. Key issues in conducting a meta-analysis of gene expression microarray datasets. *PLoS Med.* **2008**, *5*, e184. [\[CrossRef\]](#) [\[PubMed\]](#)
23. Shippey, R.; Sendera, T.J.; Lockner, R.; Palaniappan, C.; Kaysser-Kranich, T.; Watts, G.; Alsobrook, J. Performance evaluation of commercial short-oligonucleotide microarrays and the impact of noise in making cross-platform correlations. *BMC Genom.* **2004**, *5*, 61. [\[CrossRef\]](#)



24. Yauk, C.L.; Berndt, M.L.; Williams, A.; Douglas, G.R. Comprehensive comparison of six microarray technologies. *Nucleic Acids Res.* **2004**, *32*, e124. [[CrossRef](#)] [[PubMed](#)]
25. Storey, J.D.; Tibshirani, R. Statistical significance for genomewide studies. *Proc. Natl. Acad. Sci. USA* **2003**, *100*, 9440–9445. [[CrossRef](#)]
26. Davies, D.L.; Bouldin, D.W. A cluster separation measure. *IEEE Trans. Pattern Anal. Mach. Intell.* **1979**, *1*, 224–227. [[CrossRef](#)] [[PubMed](#)]
27. Zhang, B.; Schmoyer, D.; Kirov, S.; Snoddy, J. Gotree machine (gotm): A web-based platform for interpreting sets of interesting genes using gene ontology hierarchies. *BMC Bioinform.* **2004**, *5*, 16.
28. Liao, Y.; Wang, J.; Jaehnig, E.J.; Shi, Z.; Zhang, B. Webgestalt 2019: Gene set analysis toolkit with revamped uis and apis. *Nucleic Acids Res.* **2019**, *47*, W199–W205. [[CrossRef](#)]
29. Wang, J.; Vasaikar, S.; Shi, Z.; Greer, M.; Zhang, B. Webgestalt 2017: A more comprehensive, powerful, flexible and interactive gene set enrichment analysis toolkit. *Nucleic Acids Res.* **2017**, *45*, W130–W137. [[CrossRef](#)]
30. Wang, J.; Duncan, D.; Shi, Z.; Zhang, B. Web-based gene set analysis toolkit (webgestalt): Update 2013. *Nucleic Acids Res.* **2013**, *41*, W77–W83. [[CrossRef](#)]
31. Zhang, B.; Kirov, S.; Snoddy, J. Webgestalt: An integrated system for exploring gene sets in various biological contexts. *Nucleic Acids Res.* **2005**, *33*, W741–W748. [[CrossRef](#)] [[PubMed](#)]
32. Lambrou, G.I.; Sdraka, M.; Koutsouris, D. The “gene cube”: A novel approach to three-dimensional clustering of gene expression data. *Curr. Bioinform.* **2019**, *14*, 721–727. [[CrossRef](#)]
33. Jiang, D.; Tang, C.; Zhang, A. Cluster analysis for gene expression data: A survey. *IEEE Trans. Knowl. Data Eng.* **2004**, *16*, 1370–1386. [[CrossRef](#)]
34. Yang, Z.R. *Machine Learning Approaches to Bioinformatics*; World Scientific: London, UK, 2010; Volume 4.
35. Zhang, A. *Advanced Analysis of Gene Expression Microarray Data*; World Scientific: London, UK, 2006.
36. Madeira, S.C.; Oliveira, A.L. Biclustering algorithms for biological data analysis: A survey. *IEEE/ACM Trans. Comput. Biol. Bioinform.* **2004**, *1*, 24–45. [[CrossRef](#)] [[PubMed](#)]
37. Kluger, Y.; Basri, R.; Chang, J.T.; Gerstein, M. Spectral biclustering of microarray data: Coclustering genes and conditions. *Genome Res.* **2003**, *13*, 703–716. [[CrossRef](#)]
38. Yin, L.; Huang, C.H.; Ni, J. Clustering of gene expression data: Performance and similarity analysis. *BMC Bioinform.* **2006**, *7* (Suppl. 4), S19. [[CrossRef](#)]
39. D’Haeseleer, P. How does gene expression clustering work? *Nat. Biotechnol.* **2005**, *23*, 1499–1501. [[CrossRef](#)]
40. Mahanta, P.; Ahmed, H.A.; Bhattacharyya, D.K.; Kalita, J.K. Triclustering in Gene Expression Data Analysis: A Selected Survey. In *Emerging Trends and Applications in Computer Science (NCETACS), Proceedings of the 2011 2nd National Conference, Meghalaya, India, 4–5 March 2011*; IEEE: Piscataway, NJ, USA, 2011; pp. 1–6.
41. Zhao, L.; Zaki, M.J. Triclust: An effective algorithm for mining coherent clusters in 3d microarray data. In *Proceedings of the 2005 ACM SIGMOD International Conference on Management of Data, Baltimore, MA, USA, 14–16 June 2005*; pp. 694–705.
42. Bhar, A.; Haubrock, M.; Mukhopadhyay, A.; Maulik, U.; Bandyopadhyay, S.; Wingender, E. Coexpression and coregulation analysis of time-series gene expression data in estrogen-induced breast cancer cell. *Algorithms Mol. Biol. AMB* **2013**, *8*, 9. [[CrossRef](#)]
43. Ciaramella, A.; Coccozza, S.; Iorio, F.; Miele, G.; Napolitano, F.; Pinelli, M.; Raiconi, G.; Tagliaferri, R. Interactive data analysis and clustering of genomic data. *Neural Netw.* **2008**, *21*, 368–378. [[CrossRef](#)]
44. Gutierrez, A.D.; Rubio-Escudero, C.; Riquelme, J.C. Triclustering on temporary microarray data using the trigen algorithm. In *Intelligent Systems Design and Applications (ISDA), Proceedings of the 2011 11th International Conference, Graz, Austria, 22–24 November 2011*; IEEE: Piscataway, NJ, USA, 2011; pp. 877–881.
45. Araújo, R.B.; Ferreira, G.H.T.; Orair, G.H.; Meira, W., Jr.; Ferreira, R.A.C.; Neto, D.O.G.; Zaki, M.J. The partricluster algorithm for gene expression analysis. *Int. J. Parallel Program.* **2008**, *36*, 226–249. [[CrossRef](#)]
46. Jiang, D.; Pei, J.; Ramanathan, M.; Tang, C.; Zhang, A. Mining coherent gene clusters from gene-sample-time microarray data. In *Proceedings of the Tenth ACM SIGKDD International Conference on Knowledge Discovery and Data Mining, Washington, DC, USA, 22–25 August 2004*; ACM: Seattle, WA, USA, 2004; pp. 430–439.
47. Tchagang, A.B.; Phan, S.; Famili, F.; Shearer, H.; Fobert, P.; Huang, Y.; Zou, J.; Huang, D.; Cutler, A.; Liu, Z.; et al. Mining biological information from 3d short time-series gene expression data: The optricluster algorithm. *BMC Bioinform.* **2012**, *13*, 54. [[CrossRef](#)] [[PubMed](#)]
48. Mankad, S.; Michailidis, G. Biclustering three-dimensional data arrays with plaid models. *J. Comput. Graph. Stat.* **2014**, *23*, 943–965. [[CrossRef](#)]
49. Li, A.; Tuck, D. An effective tri-clustering algorithm combining expression data with gene regulation information. *Gene Regul. Syst. Biol.* **2009**, *3*, 49–64. [[CrossRef](#)] [[PubMed](#)]
50. Jain, A.K.; Murty, M.N.; Flynn, P.J. Data clustering: A review. *Acm Comput. Surv. (Csur)* **1999**, *31*, 264–323. [[CrossRef](#)]
51. Jain, A.K. Data clustering: 50 years beyond k-means. *Pattern Recognit. Lett.* **2010**, *31*, 651–666. [[CrossRef](#)]
52. Lu, C.; Ghoman, S.K.; Cutumisu, M.; Schmölder, G.M. Unsupervised machine learning algorithms examine healthcare providers’ perceptions and longitudinal performance in a digital neonatal resuscitation simulator. *Front. Pediatrics* **2020**, *8*, 544. [[CrossRef](#)]



53. Maleki, F.; Ovens, K.; Najafian, K.; Forghani, B.; Reinhold, C.; Forghani, R. Overview of machine learning part 1: Fundamentals and classic approaches. *Neuroimaging Clin. N. Am.* **2020**, *30*, e17–e32. [\[CrossRef\]](#)
54. Qi, G.J.; Zhang, L.; Lin, F.; Wang, X. Learning generalized transformation equivariant representations via autoencoding transformations. *IEEE Trans. Pattern Anal. Mach. Intell.* **2020**. [\[CrossRef\]](#)
55. Rabaglino, M.B.; Kadarmideen, H.N. Machine learning approach to integrated endometrial transcriptomic datasets reveals biomarkers predicting uterine receptivity in cattle at seven days after estrous. *Sci. Rep.* **2020**, *10*, 16981. [\[CrossRef\]](#)
56. Breheny, P.; Stromberg, A.; Lambert, J. P-value histograms: Inference and diagnostics. *High-Throughput* **2018**, *7*, 23. [\[CrossRef\]](#)
57. Dimitri, G.M.; Spasov, S.; Duggento, A.; Passamonti, L.; Lio, P.; Toschi, N. Unsupervised stratification in neuroimaging through deep latent embeddings. In *Annual International Conference of the IEEE Engineering in Medicine and Biology Society, Proceedings of the IEEE Engineering in Medicine and Biology Society, Annual International Conference, Milano, Italy, 20 July 2020*; IEEE: Piscataway, NJ, USA, 2020; pp. 1568–1571.
58. Praiss, A.M.; Huang, Y.; St Clair, C.M.; Tergas, A.I.; Melamed, A.; Khoury-Collado, F.; Hou, J.Y.; Hu, J.; Hur, C.; Hershman, D.L.; et al. Using machine learning to create prognostic systems for endometrial cancer. *Gynecol. Oncol.* **2020**. [\[CrossRef\]](#) [\[PubMed\]](#)
59. Wu, H.; Gole, R.; Ghosh, S.; Basu, A. Alternative techniques for breast tumour detection using ultrasound. In *Annual International Conference of the IEEE Engineering in Medicine and Biology Society, Proceedings of the IEEE Engineering in Medicine and Biology Society, Annual International Conference, Milano, Italy, 20 July 2020*; IEEE: Piscataway, NJ, USA, 2020; pp. 2047–2050.
60. Zhu, Z.; Cao, Y.; Qin, C.; Rao, Y.; Ni, D.; Wang, Y. Unsupervised 3d end-to-end deformable network for brain mri registration. In *Annual International Conference of the IEEE Engineering in Medicine and Biology Society, Proceedings of the IEEE Engineering in Medicine and Biology Society, Annual International Conference, Milano, Italy, 20 July 2020*; IEEE: Piscataway, NJ, USA, 2020; pp. 1355–1359.
61. Arbelaiz, O.; Gurrutxaga, I.; Muguerza, J.; Perez, J.M.; Perona, I. An extensive comparative study of cluster validity indices. *Pattern Recognit.* **2013**, *46*, 243–256. [\[CrossRef\]](#)
62. Paul, D.; Ghorai, S.; Dinesh, U.S.; Shetty, P.; Chattopadhyay, S.; Santra, M.K. Cdc20 directs proteasome-mediated degradation of the tumor suppressor smar1 in higher grades of cancer through the anaphase promoting complex. *Cell Death Dis.* **2017**, *8*, e2882. [\[CrossRef\]](#)
63. Choi, J.W.; Kim, Y.; Lee, J.H.; Kim, Y.S. High expression of spindle assembly checkpoint proteins cdc20 and mad2 is associated with poor prognosis in urothelial bladder cancer. *Virchows Arch. Int. J. Pathol.* **2013**, *463*, 681–687. [\[CrossRef\]](#) [\[PubMed\]](#)
64. Xu, Y.; Wu, G.; Li, J.; Li, J.; Ruan, N.; Ma, L.; Han, X.; Wei, Y.; Li, L.; Zhang, H.; et al. Screening and identification of key biomarkers for bladder cancer: A study based on tcga and geo data. *Biomed Res. Int.* **2020**, *2020*, 8283401. [\[CrossRef\]](#) [\[PubMed\]](#)
65. Kidokoro, T.; Tanikawa, C.; Furukawa, Y.; Katagiri, T.; Nakamura, Y.; Matsuda, K. Cdc20, a potential cancer therapeutic target, is negatively regulated by p53. *Oncogene* **2008**, *27*, 1562–1571. [\[CrossRef\]](#) [\[PubMed\]](#)
66. Wang, L.; Zhang, J.; Wan, L.; Zhou, X.; Wang, Z.; Wei, W. Targeting cdc20 as a novel cancer therapeutic strategy. *Pharmacol. Ther.* **2015**, *151*, 141–151. [\[CrossRef\]](#)
67. Dudderidge, T.; Stockley, J.; Nabi, G.; Mom, J.; Umez-Eronini, N.; Hrouda, D.; Cresswell, J.; McCracken, S.R.C. A novel, non-invasive test enabling bladder cancer detection in urine sediment of patients presenting with haematuria—a prospective multicentre performance evaluation of adxbladder. *Eur. Urol. Oncol.* **2020**, *3*, 42–46. [\[CrossRef\]](#)
68. Stoeber, K.; Swinn, R.; Prevost, A.T.; de Clive-Lowe, P.; Halsall, I.; Dilworth, S.M.; Marr, J.; Turner, W.H.; Bullock, N.; Doble, A.; et al. Diagnosis of genito-urinary tract cancer by detection of minichromosome maintenance 5 protein in urine sediments. *J. Natl. Cancer Instig.* **2002**, *94*, 1071–1079. [\[CrossRef\]](#)
69. Kelly, J.D.; Dudderidge, T.J.; Wollenschlaeger, A.; Okoturo, O.; Burling, K.; Tulloch, F.; Halsall, I.; Prevost, T.; Prevost, A.T.; Vasconcelos, J.C.; et al. Bladder cancer diagnosis and identification of clinically significant disease by combined urinary detection of mcm5 and nuclear matrix protein 22. *PLoS ONE* **2012**, *7*, e40305. [\[CrossRef\]](#) [\[PubMed\]](#)
70. Proctor, I.; Stoeber, K.; Williams, G.H. Biomarkers in bladder cancer. *Histopathology* **2010**, *57*, 1–13. [\[CrossRef\]](#) [\[PubMed\]](#)
71. Butt, E.; Ebbing, J.; Bubendorf, L.; Ardelt, P. Influence of hematuria and infection on diagnostic accuracy of urinary lasp1: A new biomarker for bladder carcinoma. *Biomark. Med.* **2017**, *11*, 347–357. [\[CrossRef\]](#) [\[PubMed\]](#)
72. Ardelt, P.; Grünemay, N.; Strehl, A.; Jilg, C.; Miernik, A.; Kneitz, B.; Butt, E. Lasp-1, a novel urinary marker for detection of bladder cancer. *Urol. Oncol.* **2013**, *31*, 1591–1598. [\[CrossRef\]](#) [\[PubMed\]](#)
73. Chiyomaru, T.; Enokida, H.; Kawakami, K.; Tatarano, S.; Uchida, Y.; Kawahara, K.; Nishiyama, K.; Seki, N.; Nakagawa, M. Functional role of lasp1 in cell viability and its regulation by micrnas in bladder cancer. *Urol. Oncol.* **2012**, *30*, 434–443. [\[CrossRef\]](#) [\[PubMed\]](#)
74. Zhang, Y.; Fang, L.; Zang, Y.; Xu, Z. Identification of core genes and key pathways via integrated analysis of gene expression and DNA methylation profiles in bladder cancer. *Med. Sci. Monit. Int. Med. J. Exp. Clin. Res.* **2018**, *24*, 3024–3033. [\[CrossRef\]](#)
75. Rubin, C.I.; Atweh, G.F. The role of stathmin in the regulation of the cell cycle. *J. Cell. Biochem.* **2004**, *93*, 242–250. [\[CrossRef\]](#)
76. Biaoxue, R.; Xiguang, C.; Hua, L.; Shuanying, Y. Stathmin-dependent molecular targeting therapy for malignant tumor: The latest 5 years' discoveries and developments. *J. Transl. Med.* **2016**, *14*, 279. [\[CrossRef\]](#)
77. Hemdan, T.; Linden, M.; Lind, S.B.; Namuduri, A.V.; Sjøstedt, E.; de Stahl, T.D.; Asplund, A.; Malmstrom, P.U.; Segersten, U. The prognostic value and therapeutic target role of stathmin-1 in urinary bladder cancer. *Br. J. Cancer* **2014**, *111*, 1180–1187. [\[CrossRef\]](#)
78. Battista, S.; Fidanza, V.; Fedele, M.; Klein-Szanto, A.J.; Outwater, E.; Brunner, H.; Santoro, M.; Croce, C.M.; Fusco, A. The expression of a truncated hmgi-c gene induces gigantism associated with lipomatosis. *Cancer Res.* **1999**, *59*, 4793–4797.

79. Chen, X.; Liu, M.; Meng, F.; Sun, B.; Jin, X.; Jia, C. The long noncoding rna hif1a-as2 facilitates cisplatin resistance in bladder cancer. *J. Cell. Biochem.* **2019**, *120*, 243–252. [\[CrossRef\]](#)
80. Lin, R.; Shen, W.; Zhi, Y.; Zhou, Z. Prognostic value of mir-26a and hmga1 in urothelial bladder cancer. *Biomed. Pharm.* **2014**, *68*, 929–934. [\[CrossRef\]](#) [\[PubMed\]](#)
81. Lin, Y.; Chen, H.; Hu, Z.; Mao, Y.; Xu, X.; Zhu, Y.; Xu, X.; Wu, J.; Li, S.; Mao, Q.; et al. Mir-26a inhibits proliferation and motility in bladder cancer by targeting hmga1. *FEBS Lett.* **2013**, *587*, 2467–2473. [\[CrossRef\]](#)
82. Qin, M.M.; Chai, X.; Huang, H.B.; Feng, G.; Li, X.N.; Zhang, J.; Zheng, R.; Liu, X.C.; Pu, C. Let-7i inhibits proliferation and migration of bladder cancer cells by targeting hmga1. *BMC Urol.* **2019**, *19*, 53. [\[CrossRef\]](#)
83. Iida, K.; Naiki, T.; Naiki-Ito, A.; Suzuki, S.; Kato, H.; Nozaki, S.; Nagai, T.; Etani, T.; Nagayasu, Y.; Ando, R.; et al. Luteolin suppresses bladder cancer growth via regulation of mechanistic target of rapamycin pathway. *Cancer Sci.* **2020**, *111*, 1165–1179. [\[CrossRef\]](#) [\[PubMed\]](#)
84. Tsai, Y.S.; Jou, Y.C.; Tsai, H.T.; Shiau, A.L.; Wu, C.L.; Tzai, T.S. Prothymosin- $\alpha$  enhances phosphatase and tensin homolog expression and binds with tripartite motif-containing protein 21 to regulate kelch-like ech-associated protein 1/nuclear factor erythroid 2-related factor 2 signaling in human bladder cancer. *Cancer Sci.* **2019**, *110*, 1208–1219. [\[CrossRef\]](#) [\[PubMed\]](#)
85. Liu, S.B.; Zhou, L.B.; Wang, H.F.; Li, G.; Xie, Q.P.; Hu, B. Loss of igf2r indicates a poor prognosis and promotes cell proliferation and tumorigenesis in bladder cancer via akt signaling pathway. *Neoplasma* **2020**, *67*, 129–136. [\[CrossRef\]](#) [\[PubMed\]](#)
86. Nord, H.; Segersten, U.; Sandgren, J.; Wester, K.; Busch, C.; Menzel, U.; Komorowski, J.; Dumanski, J.P.; Malmström, P.U.; de Ståhl, T.D. Focal amplifications are associated with high grade and recurrences in stage ta bladder carcinoma. *Int. J. Cancer* **2010**, *126*, 1390–1402. [\[CrossRef\]](#)
87. Morra, F.; Merolla, F.; Criscuolo, D.; Insabato, L.; Giannella, R.; Ilardi, G.; Cerrato, A.; Visconti, R.; Staibano, S.; Celetti, A. Cdc6 and usp7 expression levels suggest novel treatment options in high-grade urothelial bladder cancer. *J. Exp. Clin. Cancer Res.* **2019**, *38*, 90. [\[CrossRef\]](#)
88. Varol, N.; Konac, E.; Bilen, C.Y. Does wnt/ $\beta$ -catenin pathway contribute to the stability of dnmt1 expression in urological cancer cell lines? *Exp. Biol. Med.* **2015**, *240*, 624–630. [\[CrossRef\]](#)
89. Agarwal, P.; Sen, A.K.; Bhardwaj, M.; Dinand, V.; Ahuja, A.; Sood, R. Study of proliferating cell nuclear antigen expression and angiogenesis in urothelial neoplasms: Correlation with tumor grade and stage. *Urol. Ann.* **2018**, *10*, 209–214. [\[CrossRef\]](#)
90. Almeida, T.C.; Guerra, C.C.C.; De Assis, B.L.G.; de Oliveira, R.D.A.S.; Garcia, C.C.M.; Lima, A.A.; da Silva, G.N. Antiproliferative and toxicogenomic effects of resveratrol in bladder cancer cells with different tp53 status. *Environ. Mol. Mutagenesis* **2019**, *60*, 740–751. [\[CrossRef\]](#) [\[PubMed\]](#)
91. Chen, X.; Wang, P.; Wang, S.; Li, J.; Ou, T.; Zeng, X. Ciz1 knockdown suppresses the proliferation of bladder cancer cells by inducing apoptosis. *Gene* **2019**, *719*, 143946. [\[CrossRef\]](#) [\[PubMed\]](#)
92. Shi, F.; Deng, Z.; Zhou, Z.; Jiang, C.Y.; Zhao, R.Z.; Sun, F.; Cui, D.; Bei, X.Y.; Yang, B.Y.; Sun, Q.; et al. Qki-6 inhibits bladder cancer malignant behaviours through down-regulating e2f3 and nf-kb signalling. *J. Cell. Mol. Med.* **2019**, *23*, 6578–6594. [\[CrossRef\]](#) [\[PubMed\]](#)
93. Tang, F.; He, Z.; Lei, H.; Chen, Y.; Lu, Z.; Zeng, G.; Wang, H. Identification of differentially expressed genes and biological pathways in bladder cancer. *Mol. Med. Rep.* **2018**, *17*, 6425–6434. [\[CrossRef\]](#) [\[PubMed\]](#)
94. Prabhu, B.; Sivakumar, A.; Sundaresan, S. Diindolylmethane and lupeol modulates apoptosis and cell proliferation in n-butyl-n-(4-hydroxybutyl) nitrosamine initiated and dimethylarsinic acid promoted rat bladder carcinogenesis. *Pathol. Oncol. Res.* **2016**, *22*, 747–754. [\[CrossRef\]](#) [\[PubMed\]](#)
95. Watanabe, F.T.; Chade, D.C.; Reis, S.T.; Piantino, C.; Dall'Oglio, M.F.; Srougi, M.; Leite, K.R. Curcumin, but not prima-1, decreased tumor cell proliferation in the syngeneic murine orthotopic bladder tumor model. *Clinics* **2011**, *66*, 2121–2124. [\[CrossRef\]](#) [\[PubMed\]](#)
96. Zhu, Z.; Xing, S.; Lin, C.; Zhang, X.; Fu, M.; Liang, X.; Zeng, F.; Lu, G.; Wu, M. Bladder cancer therapy using combined proliferating cell nuclear antigen antisense oligonucleotides and recombinant adenovirus p53. *Chin. Med. J.* **2003**, *116*, 1860–1863.
97. Burns, M.B.; Temiz, N.A.; Harris, R.S. Evidence for apobec3b mutagenesis in multiple human cancers. *Nat. Genet.* **2013**, *45*, 977–983. [\[CrossRef\]](#)
98. Christofi, T.; Zaravinos, A. Rna editing in the forefront of epitranscriptomics and human health. *J. Transl. Med.* **2019**, *17*, 319. [\[CrossRef\]](#)
99. Yu, Q.; Chen, D.; König, R.; Mariani, R.; Unutmaz, D.; Landau, N.R. Apobec3b and apobec3c are potent inhibitors of simian immunodeficiency virus replication. *J. Biol. Chem.* **2004**, *279*, 53379–53386. [\[CrossRef\]](#)
100. Delebecque, F.; Suspène, R.; Calattini, S.; Casartelli, N.; Saïb, A.; Froment, A.; Wain-Hobson, S.; Gessain, A.; Vartanian, J.P.; Schwartz, O. Restriction of foamy viruses by apobec cytidine deaminases. *J. Virol.* **2006**, *80*, 605–614. [\[CrossRef\]](#)
101. Zielonka, J.; Bravo, I.G.; Marino, D.; Conrad, E.; Perković, M.; Battenberg, M.; Cichutek, K.; Münk, C. Restriction of equine infectious anemia virus by equine apobec3 cytidine deaminases. *J. Virol.* **2009**, *83*, 7547–7559. [\[CrossRef\]](#) [\[PubMed\]](#)
102. Harris, R.S.; Bishop, K.N.; Sheehy, A.M.; Craig, H.M.; Petersen-Mahrt, S.K.; Watt, I.N.; Neuberger, M.S.; Malim, M.H. DNA deamination mediates innate immunity to retroviral infection. *Cell* **2003**, *113*, 803–809. [\[CrossRef\]](#)
103. Zou, J.; Wang, C.; Ma, X.; Wang, E.; Peng, G. Apobec3b, a molecular driver of mutagenesis in human cancers. *Cell Biosci.* **2017**, *7*, 29. [\[CrossRef\]](#) [\[PubMed\]](#)
104. Kuong, K.J.; Loeb, L.A. Apobec3b mutagenesis in cancer. *Nat. Genet.* **2013**, *45*, 964–965. [\[CrossRef\]](#) [\[PubMed\]](#)

105. Periyasamy, M.; Singh, A.K.; Gemma, C.; Kranjec, C.; Farzan, R.; Leach, D.A.; Navaratnam, N.; Palinkas, H.L.; Vertessy, B.G.; Fenton, T.R.; et al. P53 controls expression of the DNA deaminase apobec3b to limit its potential mutagenic activity in cancer cells. *Nucleic Acids Res.* **2017**, *45*, 11056–11069. [[CrossRef](#)] [[PubMed](#)]
106. Matsumoto, T.; Shirakawa, K.; Yokoyama, M.; Fukuda, H.; Sarca, A.D.; Koyabu, S.; Yamazaki, H.; Kazuma, Y.; Matsui, H.; Maruyama, W.; et al. Protein kinase a inhibits tumor mutator apobec3b through phosphorylation. *Sci. Rep.* **2019**, *9*, 8307. [[CrossRef](#)]
107. Vasudevan, A.A.J.; Kreimer, U.; Schulz, W.A.; Krikoni, A.; Schumann, G.G.; Haussinger, D.; Munk, C.; Goering, W. Apobec3b activity is prevalent in urothelial carcinoma cells and only slightly affected by line-1 expression. *Front. Microbiol.* **2018**, *9*, 2088. [[CrossRef](#)]
108. Paraskevopoulou, V.; Papafotiou, G.; Klinakis, A. Krt14 marks bladder progenitors. *Cell Cycle* **2016**, *15*, 3161–3162. [[CrossRef](#)]
109. Papafotiou, G.; Paraskevopoulou, V.; Vasilaki, E.; Kanaki, Z.; Paschalidis, N.; Klinakis, A. Krt14 marks a subpopulation of bladder basal cells with pivotal role in regeneration and tumorigenesis. *Nat. Commun.* **2016**, *7*, 11914. [[CrossRef](#)]
110. Volkmer, J.P.; Sahoo, D.; Chin, R.K.; Ho, P.L.; Tang, C.; Kurtova, A.V.; Willingham, S.B.; Pazhanisamy, S.K.; Contreras-Trujillo, H.; Storm, T.A.; et al. Three differentiation states risk-stratify bladder cancer into distinct subtypes. *Proc. Natl. Acad. Sci. USA* **2012**, *109*, 2078–2083. [[CrossRef](#)] [[PubMed](#)]